



# Design and Implementation of a Multifunctional Screw Disassembly Workstation

Shengmin Zhang<sup>1</sup>, Yisheng Zhang<sup>1</sup>, Zhigang Wang<sup>2</sup>, Hengwei Zhang<sup>1</sup>, Kai Gu<sup>1</sup>,  
Yanlong Peng<sup>1</sup>, and Ming Chen<sup>1</sup>(✉)

<sup>1</sup> School of Mechanical Engineering, Shanghai Jiaotong University, Shanghai, China  
mingchen@sjtu.edu.cn

<sup>2</sup> Intel Labs China, Beijing, China

**Abstract.** The rapid growth of the electric vehicle industry has created a significant demand for the recycling of end-of-life electric vehicle batteries (EOL-EVB). Manual disassembly methods suffer from low efficiency, highlighting the urgent need for intelligent disassembly solutions for electric vehicle batteries. A major challenge in intelligent disassembly is dealing with uncertainty, especially when it comes to the disassembly of screws, which vary in shape, size, and rust level. To address this challenge, we present a multifunctional screw disassembly workstation specifically designed for the disassembly of screws, which constitutes a substantial portion of the EOL-EVB disassembly process. The workstation incorporates an automated sleeve replacement device that can seamlessly replace and disassemble sleeves during disassembly. Additionally, we propose a screw-type recognition method based on attributes, enabling the identification of various screw attributes to determine appropriate disassembly methods. This method exhibits scalability and requires only a small amount of data. By expanding the capabilities of our previous Neurosymbolic TAMP (Task and Motion Planning) work, we can support multiple types of screw disassembly and integrate it into the overall process of EOL-EVB disassembly, significantly reducing repetitive tasks such as screw disassembly during the disassembly process. Experimental results demonstrate the effectiveness of the workstation in disassembling multiple types of screws within a realistic disassembly environment.

**Keywords:** EOL-EVB · automatic disassembly · sleeve replacement device · recognition · attributes · NeuroSymbolic TAMP

## 1 Introduction

The disassembly of end-of-life electric vehicle batteries (EOL-EVB) presents an opportunity for resource reuse and recycling, which can help reduce the demand for new resources, environmental pollution, and resource waste. Additionally, recycling rare metals and other valuable materials from EOL-EVB can provide necessary raw materials for manufacturing new batteries. According to a report by Deloitte - a market research and consulting firm - the global electric vehicle battery recycling market is expected to grow from 5.5 billion yuan in 2021 to 299.7 billion yuan in 2028, with a compound annual growth rate of 55.92% [1]. This suggests a promising future for the recycling of

discarded electric vehicle batteries. With the increasing number of electric vehicles, the recycling and reuse of EOL-EVB will become an increasingly important issue.

Currently, manual disassembly is the primary method for disassembling EOL-EVB [2]. The main reason is that EOL-EVBs come in various brands, models, and specifications, which require different processing methods depending on the specific situation. Furthermore, the use process of EOL-EVB can cause significant changes, further increasing the uncertainty during the disassembly process. Even the simple task of disassembling screws can be challenging due to uncertainty. If the EOL-EVB has undergone deformation, the screw's position cannot be determined based on the existing battery model. If the EOL-EVB had been repaired before being scrapped, the screw type might have been changed. Similar issues exist, and they represent significant obstacles to achieving automated disassembly using robots. Some existing research has developed customized systems. Due to a lack of autonomy, they are only suitable for static environments (clean, non-deformable, and specific types of batteries) [3,4].

In the field of intelligent disassembly, the existing methods proposed mainly focus on task planning. Among them, one research [5,6] is based on a cognitive robot system to realize the disassembly of products. The system is equipped with four cognitive functions: reasoning, execution monitoring, learning, and revision. Another research [7] proposed an intelligent disassembly system based on intelligent vision, which incorporates image processing, machine learning, close loop control, multi-agent, and disassembly planning. Munir merdan et al. Proposed an ontology based automatic disassembly system [8], which couples the ontology with visual information to dynamically determine the disassembly action of the robot to achieve more flexible action. However, these methods often can not meet higher requirements for the accuracy of disassembly and can not complete the disassembly of small objects (such as screws).

In the past, there were also many studies on accurate positioning and disassembly. Such as adjusting the posture of an object using tactile feedback to achieve a desired nesting task [9,10]. Another study [11] uses the moment probability function to match the object surface and the finger surface through the object point cloud map to achieve accurate grasping. Alireza rastegarpanah et al. [12] determine the position and attitude of objects through model-based feature matching, but these methods do not apply to small objects and flexible end effectors. In addition, Li Xinyu et al. [13] utilized Faster R-CNN (high-performance deep learning algorithm) and innovative Rotating Edge Similarity (RES) algorithm to achieve high-precision positioning and classification of screws, but due to the long computational time, it is not suitable for actual disassembly tasks. Some studies [14–16] use target recognition based on grayscale values and contours to detect screws or use grayscale maps, depth maps, and HSV values to detect screws. These methods have improved the positioning accuracy of screws to a certain extent, but they cannot accurately classify various attributes such as the shape and rust of screws, and cannot be effectively applied in actual disassembly tasks.

The peak of EOL-EVB disposal is imminent, and automated disassembly of EOL-EVB is urgently needed. In our previous work, we successfully completed the continuous disassembly of a single screw in the battery pack using the framework of Neurosymbolic TAMP, introducing neural predicates and action primitives [17,18]. In this paper, we focus on the task of screw disassembly, which accounts for 40% of the disassembly work [19,20], and design a multi-functional screw disassembly workstation. This

workstation has customized end effectors and sleeve replacement devices, enabling it to disassemble various types of screws at the mechanism level. In addition, force feedback devices and visual perception modules provide multimodal sensing capabilities for workstations and propose attribute based screw-type recognition methods. Additionally, force feedback devices and visual perception modules provides the workstation with multi-modal sensing capabilities. Most importantly, we establish a neural-symbolic planning system that significantly enhances the robot's intelligence, ensuring efficient and accurate completion of the screw disassembly task.

In summary, this paper introduces three key innovative contributions: 1. Expansion of NeuroSymbolic TAMP: Building upon the original NeuroSymbolic Task and Motion Planning (TAMP) framework, this study extends its capabilities to support multiple types of screws. This advancement significantly broadens the potential applications of this method in battery disassembly and related processes.

2. Development of a Reliable Screw Replacement Mechanism: A novel screw replacement mechanism has been designed and implemented, ensuring continuous and stable operation. This mechanism holds promise for application in various screw-related tasks beyond the scope of this study.

3. Attribute-based Screw Type Recognition Method: A screw-type recognition method based on attributes is proposed, which exhibits scalability and requires minimal data. The effectiveness of this method will be further evaluated in subsequent research and development, specifically for industrial part recognition tasks.

Overall, these innovations contribute to advancing intelligent disassembly processes, expanding the capabilities of existing frameworks, and providing practical solutions for screw-related tasks in battery disassembly and beyond.

## 2 Screw Disassembly Workstation

This workstation aims to achieve rapid disassembly of various types of screws through autonomous motion planning and manipulation of robots to improve work efficiency. The main structure of the workstation is divided into a task planning layer, a multimodal sensing layer, and a mechanical structure layer. Figure 1 shows the main structure of the workstation. This workstation supports disassembling screws of various shapes and specifications. The operator only needs to place the parts to be disassembled on the workstation, and the system will automatically carry out disassembly planning; The visual perception module installed on the robot will automatically find the position of the screws and classify them; In order to adapt to various types of screws, the workstation is equipped with various types of disassemblers. When the workstation finds that the types of screws do not match, it will automatically replace the corresponding disassembler to ensure smooth disassembly; The robot is equipped with a force feedback device that can adjust the splicing action based on the shape of the screw and the force feedback of the current splicing situation, thereby achieving more accurate disassembly operations. For some severely corroded screws, conventional disassembly methods may not be effective. This workstation can perform special treatments based on the situation of the screws, such as using a power saw or milling cutter for destructive disassembly or using methods such as electrolytic rust removal, to facilitate disassembly.

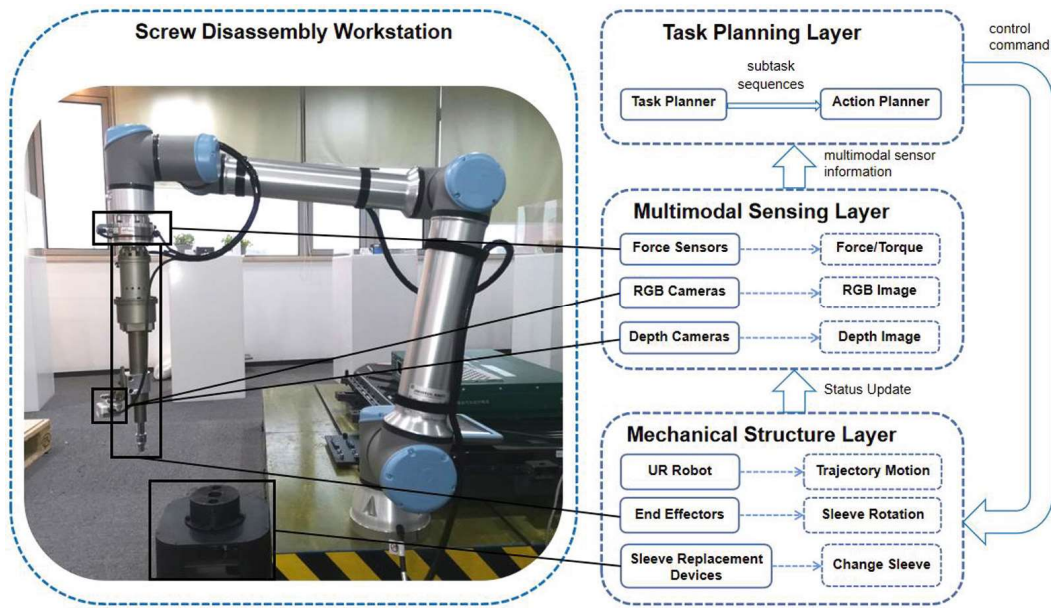


**Fig. 1.** The main structure of the workstation: 1) task planning layer. 2) multimodal sensing layer. 3) mechanical structure layer.

In summary, this workstation has the characteristics of intelligence and efficiency, which can adapt to various types of screw disassembly, and can perform fine processing for different situations.

## 2.1 Task Planning Layer

The task planning layer includes a task planner and an action planner. The task planner obtains disassembly environment information through multimodal perception, generates subtask execution sequences based on the current disassembly environment and disassembly tasks, and corrects subsequent subtask execution sequences based on the real-time disassembly environment during the subtask execution process, improving the efficiency and success rate of disassembly; The action planner generates a robot action trajectory based on the generated subtasks and combines multimodal perceptual information to drive the robot to execute.

## 2.2 Multimodal Sensing Layer

The multimodal sensing layer consists of a variety of sensors, including RGB cameras, depth cameras, and force sensors. The RGB camera and depth camera are Realsense D435, which are installed on the end effector and can obtain RGB image information and depth image information of the area in front of the end effector during robot movement; The six-dimensional pose of the target in three-dimensional space relative to the robot base coordinates is obtained by fusing multiple image information obtained in real-time, providing a basis for subsequent task planning and action planning. The force sensor uses ATI multi-axis force/torque sensors, which can measure and output forces and torque at various coordinates in the Cartesian rectangular coordinate system; Real-time detection of the forces and torque applied to the end effector during the robot's movement corrects the robot's movement and better realizes the disassembly action.

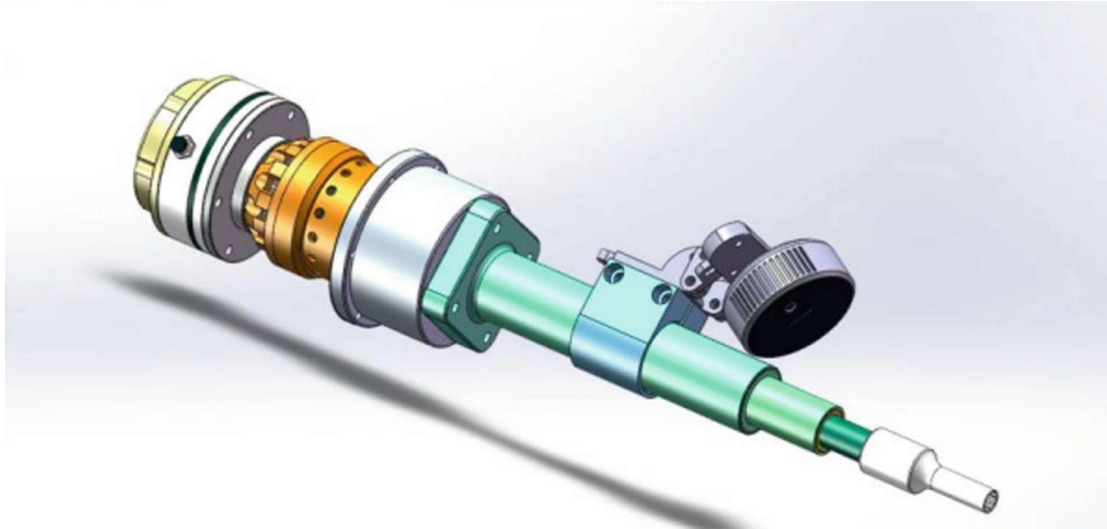


**Fig. 2.** End effector.

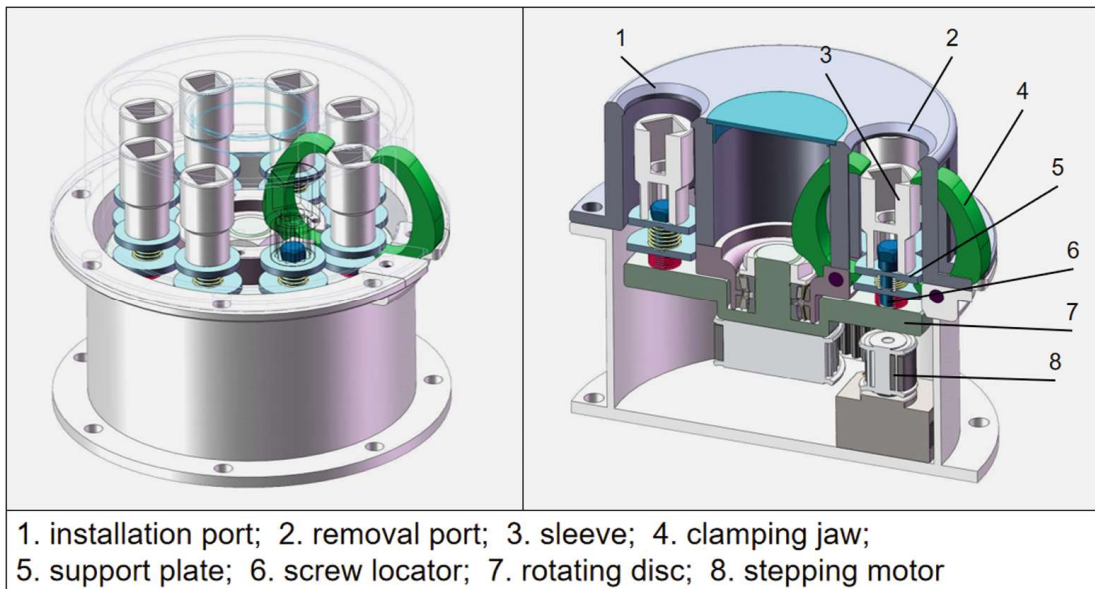


**Fig. 3.** Sleeve replacement devices.

### 2.3 Mechanical Structure Layer

The mechanical structure layer mainly includes end effectors and sleeve replacement devices. The main mechanical structure is shown in Fig. 2 and Fig. 3. The end effector is a screw disassembler driven by a motor to drive the sleeve rod and sleeve to rotate to complete the screw disassembly; The sleeve rod is connected to the main body of the disassembler by a spring, providing passive flexibility in the vertical direction for the end effectors. At the same time, the sleeve rod is flexibly connected to provide passive flexibility in the horizontal direction for the socket connection. These designs reduce the accuracy requirements required for the end effectors during the screw socket connection process.

In order to adapt to various screw disassembly tasks, it is necessary to design a sleeve replacement device for the workstation, which is mainly composed of a rotating disc carrying multiple sleeves, a stepping motor, a clamping jaw, and a housing. There is a sleeve removal position and a sleeve installation position on the housing. The motor drives the sleeve disk to rotate the required sleeve to the desired position. When it is necessary to remove the sleeve, insert the end effectors with the sleeve into the sleeve removal position. Press to make the left and right clamping jaws tightly grasp the sleeve to fix it, and lift the end effectors to separate the sleeve rod from the end effectors; When a new sleeve needs to be installed later, insert the end effectors into the sleeve mounting position, and press to connect the end effectors to the sleeve to complete the installation of the new sleeve.

When it is necessary to disassemble severely rusted screws, it is not possible to use sleeve rotation for disassembly. At this time, a milling cutter disassembler needs to be designed to grind the rusted screws flat and complete the disassembly.

When it is necessary to disassemble screws without a suitable disassembly sleeve, it is not possible to disassemble them. Instead, a power saw disassembler needs to be designed to cut a groove in the screw and then use a slotted screw sleeve for disassembly.

### 3 Disassembly Implementation Details

#### 3.1 Task Planning

**NeuroSymbolic TAMP.** The advantages of NeuroSymbolic TAMP lie in its interpretability, learnability, and extensibility. By introducing neural predicates, the system can abstract and represent the features of small fastener disassembly. At the same time, the continuous optimization and expansion of action primitives also enable the system to adapt to more complex disassembly tasks.

When applied to screw disassembly, the system can sense the disassembly environment through multimodal sensors, and use NeuroSymbolic to abstract information such as the position, shape, and characteristics of screws into understandable symbolic forms, thereby avoiding the use of complex methods to identify screw features. By generating action primitive sequences that conform to logical reasoning, the system can directly drive the robot to complete the disassembly task. The training and enhancement of neural predicates and the expansion and optimization of action primitives enable the system to better adapt to different types of screws, thereby improving the accuracy and efficiency of disassembly. In previous work, the advantages of NeuroSymbolic TAMP in disassembling small fasteners in unstructured environments have also been verified [17].

**Neural Predicates and Action Primitives.** In previous work, two neural predicates, “target\_aim()” and “target\_clear()”, was defined to determine whether the end effector is consistent with the position and posture of the target object and whether there are obstacles around or above the target object. At the same time, eight action primitives are defined, including “Approach”, “Mate”, “Push”, “Insert”, “Fumble”, “Search”, “Re insert”, and “Disassemble”. This intelligent disassembly system can achieve continuous and stable disassembly of a single type of screw, but in reality, there are many

**Table 1.** Description of Disassembly Primitives

Primitive	Pre-condition	Result	Function Description
Recognize	<ol style="list-style-type: none"> <li>1. The sleeve is aligned with the screw;</li> <li>2. There are no obstacles near the screw.</li> </ol>	<ol style="list-style-type: none"> <li>1. The system has completed screw type identification;</li> <li>2. The system completes the identification of the degree of screw corrosion;</li> <li>3. The screw type matches the sleeve type.</li> <li>4. There is matching sleeve in the sleeve replacement device</li> </ol>	This primitive identifies the type, specification, and degree of corrosion of the screw currently being disassembled. Determine if there is a matching sleeve in the sleeve replacement device.
Change	<ol style="list-style-type: none"> <li>1. The system has completed screw type identification;</li> <li>2. The screw type does not match the sleeve type;</li> <li>3. There is a matching sleeve in the sleeve replacement device.</li> </ol>	<ol style="list-style-type: none"> <li>1. The screw type matches the sleeve type.</li> </ol>	This primitive drives the robotic arm to replace a sleeve that matches the current screw shape and specification.
Cut	<ol style="list-style-type: none"> <li>1. The system has completed screw type identification;</li> <li>2. There is no matching sleeve in the sleeve replacement device.</li> </ol>	<ol style="list-style-type: none"> <li>1. The screw type changed to a flat-head screw.</li> </ol>	This primitive cuts screws without matching sleeves into slotted screws.
Mill	<ol style="list-style-type: none"> <li>1. The system has completed the identification of the degree of screw corrosion;</li> <li>2. The target screw is severely rusted.</li> </ol>	<ol style="list-style-type: none"> <li>1. The screw disassembly is completed.</li> </ol>	This primitive grind the severely rusted screws flat.

**Table 2.** Description of Predicates

Predicate	Function Description
target_match(senor)	This neural predicate means that the shape and specification of the current screw can be disassembled using the currently equipped sleeve.
exist_sleeve(senor)	This neural predicate means that there is a matching disassembly sleeve for the current screw.
target_rust(senor)	This neural predicate means that the degree of rust on the screw is very severe.

types of screws in disassembly work, with different shapes and sizes. A disassembly workbench that can only disassemble a single screw cannot be extended to a real disassembly operation. To solve this problem, We have added the neural predicate “target\_match()”, “exist\_sleeve()” and “target\_rust()” to determine whether the current target screw matches the currently assembled disassembler, whether there is a matching sleeve, and whether there is excessive rust. Four action primitives, “Recognize”, “Change”, “Cut” and “Mill”, are newly defined to identify the feature type of the current target screw, drive the robot to automatically replace the disassembler when the disassembler and target screw types are inconsistent, cut screws without matching sleeves and grind down severely rusted screws.

The definition of its action primitive is shown in the following Table 1.

The implementation of the action primitive “Recognize” is to move the end effector to a position 20 mm directly above the target screw, acquire the RGB image captured by the camera at the current position, and input it into the YOLO network. The YOLO network is a screw position recognition network whose main functions are to obtain the center position of the positioning frame, the size of the positioning frame, and the captured screw image of the target screw. Then input the captured screw image into the VAE network to determine the shape attributes of the current target screw, and combine the size of the positioning frame to obtain the size of the screw to comprehensively determine the specific model of the screw. Compare the type of the target screw with the sleeve type on the current end effector: If the type matches, set “target\_match()” to True; If the types do not match, set “target\_match()” to False (Table 2).

**Implementation of the “Change” Primitive.** When executing the action primitive “Change”, we need to input the current end effector position, current sleeve type, and target sleeve type. In order to allow the end effector to be vertically inserted into the sleeve replacement device, two pre-replacement positions have been set, which are located 20 mm above the sleeve installation and removal port. Firstly, place the current sleeve back into the sleeve replacement device, drive the stepping motor to rotate the rotating disc and move the current sleeve placement position below the removal port, move the end effector from its initial position to the pre-replacement position at the removal port, and insert it vertically downwards into the removal port. At this time, the sleeve contacts the screw locator and compresses the spring in the end effector, Drive the end effector motor to rotate slightly so that the notch under the sleeve matches the shape of the screw locator. The spring in the end effector is released and pressed down on the sleeve and support plate (supported by a spring between the support plate and the rotating disc). The support plate presses down on the lower part of the clamping claw, causing the clamping claw to tighten in the middle and make contact with the upper part of the sleeve. At this time, move the end effector upwards to remove the current sleeve; The next step is to install the target sleeve. Drive the stepping motor to rotate the rotating disc and move the target sleeve below the installation port, move the end effector to the pre-replacement position at the installation port, and vertically insert it into the installation port. At this time, the empty rod contacts and compresses the target sleeve, causing the spring in the end effector to compress. driving the end effector motor to rotate slightly to fit the shape of the gap on the rod and sleeve, The spring release in the end effector compresses and installs the sleeve onto the end effector, and then moves back to the initial position to complete an automatic replacement of the sleeve. Update the current casing type in the planner and set “target\_match()” to True.

**Execution Flow Chart.** Firstly, when obtaining a rough positioning position of the screw to be disassembled, the execution action primitive “Approach” moves to the vicinity above the screw; When there are obstacles around the target screw, execute the action primitive “Push” to clear the obstacles; When the end effector is not aligned with the target screw, execute the action primitive “Mate” to align it; When there are no obstacles around the target screw and the end effector is aligned with the target screw, the execution action primitive “Recognize” identifies the current screw type and spec-



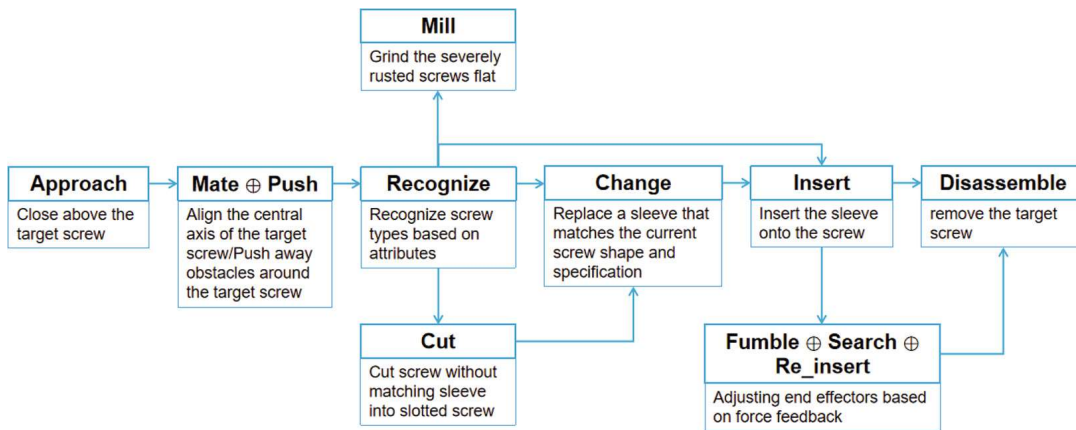


**Fig. 4.** Execution Flow Chart.

ification; When the screw type and specification do not match the sleeve, execute the action primitive “Change” to replace the appropriate sleeve; When the screw type and specification match the sleeve, execute the action primitive “Insert”; According to the force feedback data during the sleeve connection, select and execute some or all of the action primitives “Fumble”, “Search”, and “Re\_insert” until the screw socket connection is successful. Execute the action primitive “Disassemble” to remove the current screw and proceed with the disassembly of the next screw. When the target screw does not have a matching sleeve during the disassembly process, execute the action primitives “Cut” to turn it into a This primitive cuts screws without matching sleeves into slotted screw and use a slotted screw sleeve for disassembly. When the target screw is severely rusted during the disassembly process, execute the action primitives “Mill” to grind it flat.

The flow diagram is shown in the Fig. 4.

### 3.2 Screw Type Recognition Based on Attribute

In contrast to conventional detection methods that directly rely on types of object detection, our approach utilizes a series of classifiers to categorize the various attributes of screws. For instance, we classified screws into four categories based on the degree of rust, ranging from “no rust” to “severe rust”. Additionally, we employed shape-based classification, distinguishing “outer hexagonal”, “inner hexagonal” and so on. This methodology offers several significant advantages:

1. Sufficient availability of training data: During the training phase of the object detection network, we found it advantageous to group all screws together and consider them as a single class. However, when training for attribute classification, we organized screws with similar attributes into distinct groups. This approach eliminated the need to partition the limited data into numerous small classes for training purposes. Importantly, our investigation revealed that subdividing the data into smaller classes would not meet our requirements within the dataset.
2. Combination of multiple attributes: By combining different attributes, we were able to infer and identify screws that were not originally present in the dataset. This capability demonstrates the versatility and robustness of our approach, enabling it

to handle screw types that were not encountered during the initial data collection phase.

**VAE Recognition Algorithm.** Our system uses VAE to classify attributes for several reasons: 1 Subsequent experiments have shown that VAE performs best in our dataset; 2. VAE facilitates the expansion of attributes in the future. For example, the degree of corrosion can be divided into no rust and severe rust. If future treatment methods require recognition of mild and moderate rust, we can generate a new classification method by defining the distance from the existing two categories without retraining this attribute.

The VAE network is an unsupervised learning network, which obtains an encoder and a decoder through training and can encode pictures into feature vectors containing their various attributes and restore them through the decoder. VAE networks can be trained with a small amount of data, and can effectively extract target attribute information such as shape, color, and state from images. Therefore, VAE networks are very suitable for classifying various small fasteners such as screws in unstructured scenes.

The conventional VAE loss function is defined as:

$$L(x) = E_{q(z|x)}[\log p(x|z)] + \beta \cdot D_{KL}(q(z|x)||p(z)) \quad (1)$$

but this loss function only focuses on the pixels of a single image and cannot effectively distinguish images with different characteristics. On this basis, we use pairs of images during training and add the relationship between images in the loss function [21]:

$$L(x_1, x_2) = (L(x_1) + L(x_2)) / 2 + aH(x_1, x_2) \quad (2)$$

$$H(x_1, x_2) = \begin{cases} \max(0, d_m - \|z_1 - z_2\|_1) & \text{similar}(x_1, x_2) \\ \|z_1 - z_2\|_1 & \text{different}(x_1, x_2) \end{cases} \quad (3)$$

where H is the feature difference between images and its weight is adjusted by the coefficient  $a$ . The hyper-parameter  $d_m$  describes the spread distance margin of the potential vector so that  $z_1$  and  $z_2$  are distributed in different regions in the potential space. This allows the VAE network to make the encoding vectors of images with the same attributes closer and images with different attributes further during training, which is more conducive to our judgment of target attributes.

**Identification of Screw Types.** Collect screw image data on the battery pack in advance, use a VAE encoder to convert it into a feature vector, cluster the screws with the same shape attributes, and calculate the average vector. After obtaining the image information of the target screw to be disassembled, it is input into the VAE encoder to obtain its feature vector. By comparing the feature vector of the target screw with the average vector of screws with different shape attributes, the closest one is the geometric shape attribute of the current target screw. Similarly, the screw status attribute can be determined. Finally, based on the size of the YOLO positioning bracket and the relative coordinate relationship between the camera and the screw, the specifications of the screw can be comprehensively determined to determine the specific model of the screw. Multiple types of screws in a real disassembly environment are shown in Fig. 5.



**Fig. 5.** Multiple types of screws in a real disassembly environment.

### 3.3 Force Feedback Adjustment of Different Screws

In our previous work, we added action primitives “Fumble”, “Search”, and “Re\_insert” to successfully implement force feedback correction if a particular type of screw cannot be successfully inserted during disassembly. But when using different disassembly sleeves to disassemble different screws, due to the different shapes and specifications of the screws, using a single force feedback correction model cannot effectively correct the deviation of the sleeve connection during the disassembly process. Therefore, we train different force feedback models based on the shapes and specifications of different screws, and change them to “Fumble (bolt\_type)”, “Search (bolt\_type)” and “Re\_insert (bolt\_type)” based on the original action primitive, select an appropriate force feedback model based on the judgment of the screw type during disassembly and invoke action primitives to correct the splicing process.

## 4 Experimental Verification

### 4.1 Accuracy and Speed of VAE Judgment

In a simulation environment, we conducted experiments on four different shapes of screws (outer hexagonal screw, inner hexagonal screw, cross screw, and star screw) with varying degrees of rust (no rust, mild rust, moderate rust, and severe rust). The trained VAE screw classification network achieved a success rate of 97.75% in identifying specific shapes of screws during actual disassembly, At the same time, the accuracy of identifying the degree of corrosion of screws has reached 100%; At the same time, we use classical image classification networks to train four classification networks for screw

**Table 3.** Success Rate of Classical Image Classification Network Detection

	shape(4class)	rust(4class)	shape&rust(16class)
VGG-16	94.84%	98.48%	89.28%
ResNet	87.87%	100%	73.7%
Mobilevit	84.84%	91.18%	89.79%
Densenet	88.18%	99.74%	82.39%
VAE	97.75%	100%	—

shape and rust degree, while training sixteen classification networks for screw shape and rust degree, with classification accuracy shown in the Table 3. In a real machine environment, the trained VAE screw classification network achieved a success rate of 100% in identifying specific screw shapes during the actual disassembly process.

Compared to classical image classification networks, VAE networks have higher classification accuracy and can perform well even in smaller datasets. Previously, we used YOLO to directly detect and classify screw types, but it was difficult for YOLO to classify multiple features of screws, and it required recalibration when adding new feature types, resulting in a large workload. In contrast, using VAE networks can complete training using smaller datasets and easily collect training data during the disassembly process without excessive processing.

#### 4.2 Success Rate of Continuous Disassembly of Multiple Screws

In the simulation environment, in the disassembly experiment of six different types of screws (M8 outer hexagon screw, M10 outer hexagon screw, M12 outer hexagon screw, inner hexagon screw, cross screw, and star screw), the recognition success rate of specific screw shape was 97.75%, and the sleeve replacement success rate was 100%. The overall continuous disassembly success rate was 97.75%. In the actual machine disassembly experiment, in the disassembly experiment of five different types of screws (M8 outer hexagon screw, M10 outer hexagon screw, M13 outer hexagon screw, M10 outer hexagon cross screw, M13 outer hexagon cross screw), the recognition success rate of the specific screw shape was 100%, and the sleeve replacement success rate was 100%. The overall continuous disassembly success rate was 100%. Related experimental videos can be found on the website <https://sites.google.com/view/disassembly-real>.

## 5 Conclusions

In order to solve the problem of screw disassembly for robots in industrial disassembly tasks, we have designed a multifunctional screw disassembly workstation. Expanding its functionality on the existing NeuroSymbolic TAMP, workstations can autonomously plan and execute action primitives based on their perception of the current environment to complete the disassembly of various screws. A sleeve replacement device has been

designed to achieve automatic sleeve replacement, which can stably achieve sleeve replacement during disassembly. When identifying screws, a screw type recognition method based on attributes has been proposed, which only requires a small amount of data and has scalability. Through experiments, we have verified that the system can recognize various screw shapes, specifications, and degrees of rusting in a simulation environment, achieving a disassembly success rate of 97.75%. Complete the identification of multiple real screw shapes and specifications in a real machine environment and achieve a 100% success rate in disassembly. However, in the real environment, the number of severely rusted screws is scarce, making it difficult to conduct experiments on them. Therefore, there is no identification of screw rust attributes and destructive disassembly experiments conducted in the real environment.

In the future, we will add more types of disassembly sleeves to complete the identification and disassembly of more types of screws and conduct destructive disassembly experiments on unmatched sleeves and severely corroded screws. The work of locating screws and obtaining screw images completed by YOLO can be completed using Segment-Anything [22], which does not require specialized training to achieve good segmentation results and fewer recognition errors. Increase mobile platforms to expand robot workspace and achieve global disassembly.

## References

1. Chris Lu, N.K.: China lithium industry Deloitte POV 3.0: sustainable future of lithium recycle. Deloitte Consulting China, Technical report 6 (2022)
2. Harper, G., et al.: Recycling lithium-ion batteries from electric vehicles. *Nature* **575**(7781), 75–86 (2019)
3. Chen, H., Shen, J.: A degradation-based sorting method for lithium-ion battery reuse. *PLoS One* **12** (2017)
4. Scrosati, B., Garche, J., Sun, Y.-K.: 20 - recycling lithium batteries. In: Scrosati, B., Garche, J., Tillmetz, W. (eds.) *Advances in Battery Technologies for Electric Vehicles*. Woodhead Publishing Series in Energy, pp. 503–516. Woodhead Publishing (2015)
5. Vongbunyong, S., Kara, S., Pagnucco, M.: Application of cognitive robotics in disassembly of products. *CIRP Ann.* **62**(1), 31–34 (2013)
6. Vongbunyong, S., Kara, S., Pagnucco, M.: Learning and revision in cognitive robotics disassembly automation. *Robot. Comput.-Integr. Manuf.* **34**, 79–94 (2015)
7. Weyrich, M., Wang, Y.: Architecture design of a vision-based intelligent system for automated disassembly of e-waste with a case study of traction batteries. In: 2013 IEEE 18th Conference on Emerging Technologies & Factory Automation (ETFAs), pp. 1–8. IEEE (2013)
8. Merdan, M., Lepuschitz, W., Meurer, T., Vincze, M.: Towards ontology-based automated disassembly systems. In: 36th Annual Conference on IEEE Industrial Electronics Society, IECON 2010, pp. 1392–1397. IEEE (2010)
9. Kim, S., Rodriguez, A.: Active extrinsic contact sensing: application to general peg-in-hole insertion. In: 2022 International Conference on Robotics and Automation (ICRA), pp. 10 241–10 247. IEEE (2022)
10. Ma, D., Dong, S., Rodriguez, A.: Extrinsic contact sensing with relative-motion tracking from distributed tactile measurements. In: 2021 IEEE International Conference on Robotics and Automation (ICRA), pp. 11 262–11 268. IEEE (2021)

11. Adjigble, M., Marturi, N., Ortenzi, V., Rajasekaran, V., Corke, P., Stolkin, R.: Model-free and learning-free grasping by local contact moment matching. In: 2018 IEEE/RSJ International Conference on Intelligent Robots and Systems (IROS), pp. 2933–2940. IEEE (2018)
12. Rastegarpanah, A., Gonzalez, H.C., Stolkin, R.: Semi-autonomous behaviour tree-based framework for sorting electric vehicle batteries components. *Robotics* **10**(2), 82 (2021)
13. Li, X., et al.: Accurate screw detection method based on faster R-CNN and rotation edge similarity for automatic screw disassembly. *Int. J. Comput. Integr. Manuf.* **34**(11), 1177–1195 (2021)
14. Bükler, U., et al.: Vision-based control of an autonomous disassembly station. *Robot. Auton. Syst.* **35**(3–4), 179–189 (2001)
15. Bdiwi, M., Rashid, A., Putz, M.: Autonomous disassembly of electric vehicle motors based on robot cognition. In: IEEE International Conference on Robotics and Automation (ICRA), pp. 2500–2505. IEEE (2016)
16. Bdiwi, M., Rashid, A., Pfeifer, M., Putz, M.: Disassembly of unknown models of electrical vehicle motors using innovative human robot cooperation. In: Proceedings of the Companion of the 2017 ACM/IEEE International Conference on Human-Robot Interaction, pp. 85–86 (2017)
17. Zhang, H., Yang, H., Wang, H., Wang, Z., Zhang, S., Chen, M.: Autonomous electric vehicle battery disassembly based on neurosymbolic computing. In: Arai, K. (ed.) *Intelligent Systems and Applications*, pp. 443–457. Springer, Cham (2023). [https://doi.org/10.1007/978-3-031-16078-3\\_30](https://doi.org/10.1007/978-3-031-16078-3_30)
18. d'Avila Garcez, A., Lamb, L.C.: Neurosymbolic AI: the 3rd wave. arXiv e-prints, pp. arXiv-2012 (2020)
19. Li, R., et al.: Unfastening of hexagonal headed screws by a collaborative robot. *IEEE Trans. Autom. Sci. Eng.* **17**(3), 1455–1468 (2020)
20. Wegener, K., Andrew, S., Raatz, A., Dröder, K., Herrmann, C.: Disassembly of electric vehicle batteries using the example of the Audi Q5 hybrid system. *Procedia CIRP* **23**, 155–160 (2014). 5th CATS 2014 - CIRP Conference on Assembly Technologies and Systems
21. Du, Y., et al.: Learning symbolic operators: a neurosymbolic solution for autonomous disassembly of electric vehicle battery. arXiv preprint [arXiv:2206.03027](https://arxiv.org/abs/2206.03027) (2022)
22. Kirillov, A., et al.: Segment anything. arXiv preprint [arXiv:2304.02643](https://arxiv.org/abs/2304.02643) (2023)